Article

Impact of Canopy Coverage and Morphological Characteristics of Trees in Urban Park on Summer Thermal Comfort Based on Orthogonal Experiment Design: A Case Study of Lvyin Park in Zhengzhou, China

Sihan Xue [1,*], Xinfeng Chao [1], Kun Wang [2,*], Jingxian Wang [2], Jingyang Xu [1], Ming Liu [1] and Yue Ma [3]

1   School of Architecture, Zhengzhou University, Zhengzhou 450001, China; chaoxinfeng@gs.zzu.edu.cn (X.C.); xjy990411@163.com (J.X.); liuming990520@163.com (M.L.)
2   College of Landscape Architecture and Art, Henan Agricultural University, Zhengzhou 450002, China; wjxwjx326@163.com
3   Department of Earth System Science, Tsinghua University, Beijing 100084, China; ma-y22@mails.tsinghua.edu.cn
*   Correspondence: xuesh@zzu.edu.cn (S.X.); wkun@henau.edu.cn (K.W.)

Abstract: As an integral part of urban forests, urban parks play a vital role in mitigating urban heat islands (UHI) and providing residents with comfortable outdoor recreational plots. For high-quality use of the trees in regulating the thermal comfort of urban parks, previous studies primarily focused on the microclimate variations caused by tree coverage and morphological features separately. However, there is still a lack of systematic understanding of how tree canopy coverage (TCC) and its morphological elements, including leaf area index (LAI), trunk height (TH), and crown diameter (CD), combined affect the thermal comfort in the urban park. This study employed an orthogonal experiment design and ENVI-met software to simulate the microclimate of various multi-factor combination models in the case of a typical urban park in a temperate continental climate zone in China, analyzing the simulated result through physiological equivalent temperature (PET). Results show that the contribution ratio of various elements to the thermal environment vary over time. In studied elements, the contribution ratio of TCC to PET is consistently higher than 50% during the morning, midday, and evening periods, reaching a peak of 67% in the evening. The maximum contribution ratios for CD, TH, and LAI occur during midday, morning, and midday, respectively, with corresponding contribution ratios of approximately 22%, 10%, and 9%, respectively. The ranking of elements affecting thermal comfort in the urban park generally is TCC, CD, LAI, TH throughout the day, apart from the morning, when the influence of TH is greater than LAI. The optimal combination of elements is 85% TCC, 4m TH, 3.9 LAI, and 7m CD, and thirteen combinations of element cases meet the thermal comfort requirements during summer. The research findings highlight the significance of optimizing the configuration of trees in creating a more comfortable and inviting space for human activities.

Keywords: greening elements; outdoor thermal comfort; software simulation; multi-factor experiment design; utilization of urban forest plant

1. Introduction

In recent years, with the rapid development of urbanization and industrialization, a large amount of green space has been continuously replaced by urban buildings, and the coverage of impermeable surfaces (such as asphalt and concrete) has also been increasing [1,2]. This has led to the accumulation of excessive heat energy within the city, causing frequent occurrences of extremely hot weather and exacerbating the urban heat island effect [3]. As a result, the incidence of heat-related illnesses is constantly increasing, especially among vulnerable populations, including the elderly and individuals with weakened immune systems.

Moreover, the risk of contracting these diseases is higher in outdoor spaces where people gather [4,5]. An urban forest can effectively mitigate the UHI effect in summer via the combined impact of shading and evapotranspiration of plants [6,7]. Urban parks, as a typical urban forest, have become important outdoor places for residents to engage in recreational activities due to their significant cooling effect [8]. Improving the thermal environment of parks can prevent heat-related health risks, increase the use of outdoor spaces, and reduce energy consumption [9–11]. However, the constantly expanding demand for built-up areas has limited the development of urban parks [12]. In order to efficiently harness the ability of urban forests to improve the urban thermal environment within limited land, it is necessary to plan urban parks strategically, particularly by maximizing the efficient utilization of trees for their regulating role [13].

Trees in parks have a better cooling effect compared to other types of plants, mainly due to the shade provided by their canopy [14]. As the tree canopy coverage (TCC) increases, the cooling and humidification effects become more pronounced [11]. Additionally, the morphological characteristics of trees also have a significant impact on their cooling effects. For example, the crown diameter (CD) and leaf area index (LAI) primarily determine the shading range and blocking capacity of the plant canopy towards solar radiation, which directly affects the amount of solar radiation reaching the ground [15]. Generally, a broad and dense tree canopy can significantly decrease the temperature under the trees, and it is a key component for trees to exert their microclimate effect [16]. Furthermore, the height of the tree trunk determines the openness of the space under the tree, which has an impact on the wind environment [16]. Therefore, if the advantages of a broad tree canopy and a tall tree trunk can be considered together when selecting tree species, it would be beneficial for creating a better microclimate during summer.

Urban forests not only have a significant effect on regulating the urban microclimate but also indirectly impact human thermal comfort. In order to quantitatively assess the impact of greening on human thermal comfort, previous studies have proposed different thermal indices, such as Physiological Equivalent Temperature (PET) [17], Predicted Mean Vote (PMV) [18], Universal Thermal Climate Index (UTCI) [19], and so on. Among them, PET has been proven to be a commonly used thermal index for evaluating human outdoor thermal sensation. Its advantage lies in the comprehensive consideration of various meteorological parameters such as air temperature (Ta) and relative humidity (RH), as well as individual parameters of humans. Additionally, the correspondence between PET and thermal sensation scales has been established, and it has been widely applied in microclimate comfort assessment [20,21]. Previous studies have demonstrated that optimizing urban greening can transform the summer thermal sensation from hot (34.92 °C) to slightly warm (26.16 °C) [22]. Taking residential green spaces, which are the most frequently used urban forests by residents, as an example, in a high-rise residential area (building height of 33 m), when the TCC ratio increases to 45%, PET during the afternoon in summer can be reduced by 10 °C [23].

In recent years, with the development of computer technology, numerical simulation techniques have been increasingly used for the analysis and prediction of thermal environments in urban forests due to their good experimental controllability. There are more and more simulation studies on how urban forests regulate urban microclimates, particularly focusing on the impact of greening elements such as TCC and plant morphological characteristics like LAI, trunk height (TH), and CD [22,23]. However, most of these studies only consider the impact of single element variations in greening on the thermal environment [24–26], neglecting the coordinated and collective effects among greening elements. Currently, there is a lack of systematic understanding regarding how the combined effect of multiple greening elements can promote thermal comfort. In this study, multiple combinations of greening elements, including TCC, TH, LAI, and CD, were established to fill the gap in comprehensive studies in this field. The Orthogonal Design of Experiments [27,28] was selected, which is a commonly used multi-element experimental method that effectively reduces the number of experimental designs and shortens the duration

of experiments. In addition, the simulation software ENVI-met was used to simulate the thermal comfort of multiple combinations of greening elements, which is widely applied in urban forest microclimate research. Taking a city in northern China as the research area, the main objective is to explore how to effectively utilize the combined effects of greening elements in urban forest to improve thermal comfort in urban areas during the summer. Specifically, the following questions need to be answered:

1. What is the potential of the tree coverage ratio and morphological characteristics in improving thermal comfort?
2. Do greening elements have different effects on thermal comfort during different periods?
3. What is the importance ranking of these four greening elements, namely TCC, TH, LAI, and CD, in regulating thermal comfort?
4. What is the optimal combination of TCC and morphological elements in improving thermal comfort during a hot summer in China?

2. Materials and Methods

2.1. Study Area

This study has chosen an urban park, Lvyin Park, as the study area in Zhengzhou, China. As shown in Figure 1a, Zhengzhou is located in the central region of the North China Plain ($31°23'–36°22'$ N, $110°21'–116°39'$ E). It possesses a monsoon-influenced humid continental climate, characterized by torridity, humidity and rainy summers with a prevailing southeasterly wind [3]. In recent years, extreme heat has occurred frequently in Zhengzhou. As of August 16th this year, the highest recorded temperature has reached 41.3 °C (on 8 July), ranking second in all of China. Furthermore, the number of days with a maximum daily temperature exceeding 35 °C has reached 28 days, far surpassing the annual average (19.3 days) of high-temperature days in Zhengzhou from 2000 to 2019 (Statistical data on high temperatures by the China Meteorological Administration, www.weather.com.cn, 17 August 2023). This extreme heat weather seriously interferes with residents' outdoor activity, damaging the thermal experience, and increasing the risk of diseases such as heliosis and cardiopathy [29].

Taking the diversity of morphological characteristics of trees, such as LAI, TH, and CD, and the convenience of carrying out the on-site measurement of microclimate into account, Lvyin Park was selected as the area for simulation experiments (Figure 1b). Meanwhile, the boundary shape of this park is a regular rectangle and the total area of the park is approximately 67,700 m^2, 83% of which is covered by greenery. Trees in the park are made up of over 80 species of temperate deciduous and evergreen forest species, totaling more than 7000 trees. These species are usually used in urban greening as well, such as *Platanus* spp., *Ligustrum lucidum*, and *Ginkgo biloba*.

2.2. Modeling Description and Validation

2.2.1. Model Configuration

ENVI-met 5.0.3 (ENVI-met GmbH, Essen, Germany) is a microclimate simulation software for three-dimensional spaces based on principles of computational fluid dynamics, thermodynamics, and urban ecology with the maximum temporal and spatial resolution of 1 s and 0.5 m, respectively [6]. This software is adept in simulating surface-plant-air interactions in different contexts, and therefore it is widely utilized in assessing the impact of landscape elements, such as vegetation and water bodies, on the thermal environment [30,31].

Before establishing the model of the study area, we conducted a field survey on 28 June 2021, to collect the morphological data of the plants. This included measurements of tree and TH, CD, LAI, as well as shrub and grass height. The tree and TH were measured using a Vertex IV hypsometer. The measurement of TH is specifically for the height below the branches. The LAI was measured using the HemiView 2.1 SR5 Plant Canopy Analyzer. The CD was measured using a portable tape, separately measuring the east-west width

and the north–south width of the canopy's vertical projection. The shrub and grass heights were also measured using the portable soft tape measure.
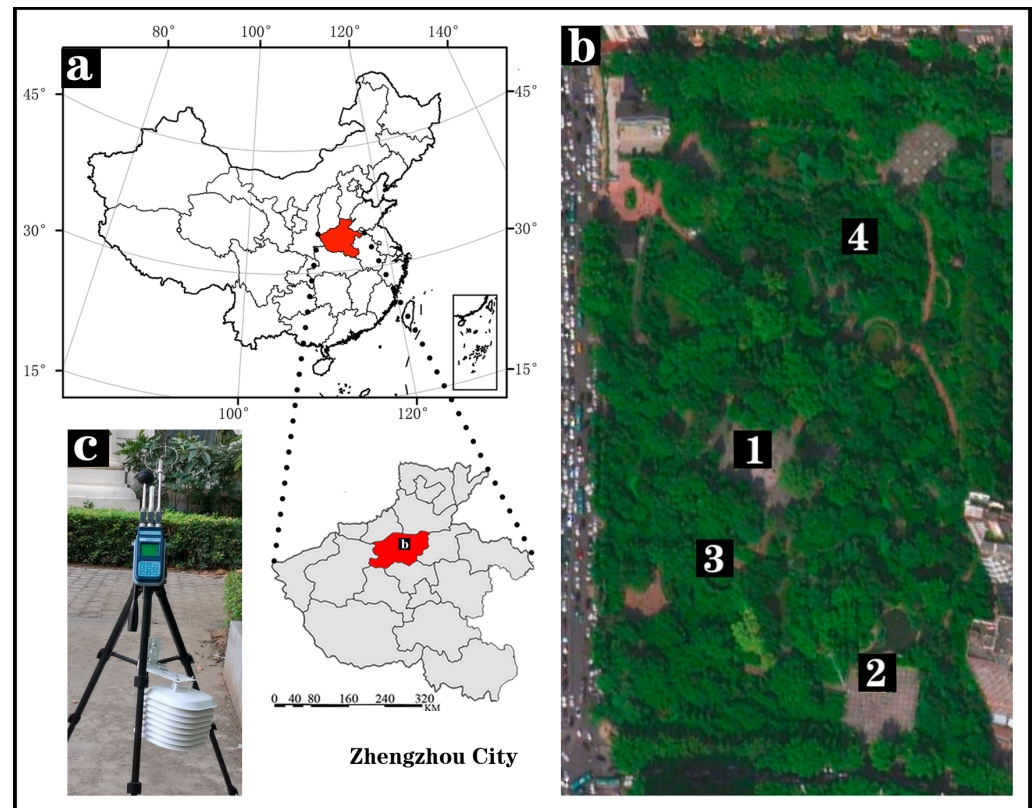
Figure 1. (**a**) Location of Zhengzhou; (**b**) Google Earth map of the study area, Lvyin Park and sample points include unshaded location (1) and (2), tree-shaded location (3) and (4); (**c**) measurement instruments.

According to the Google Earth map and field survey, the model of the actual scenario of the study area, Lvyin Park, was set up at a resolution of 5 m in both horizontal and vertical directions in ENVI-met. In this study, the park was modeled in a horizontal area of 200 × 350 m, composed of 40 × 70 cell grids in the actual scenario. The total number of cell grids in the vertical direction was 20, indicating the spatial height of this model was 100 m. To avoid the boundary effect for ENVI-met modeling, this study added 30 nesting grids (i.e., 150 m) around the domain of the park, which were more than the nesting grids in previous related studies [32,33]. Given over 80 plant species in the park, the plants were roughly represented by the models in the ENVI-met database, the morphological characteristics of which were closely approximated to the real species as much as possible. The hard pavement, apart from the green underlayment, was set as impermeable concrete.

The specific parameters were input to initialize the simulation model (Table 1). We chose 28 June 2021 as the simulated day, which is close to the peak heat level during the summer in Zhengzhou. The meteorological data of this day were applied as the boundary conditions of the model in the "Simple Forcing" scheme. The background meteorological data and soil data were retrieved from Zhengzhou (57,083) Weather Station. The simulation lasted 24 h from 0:00 to 23:59. Other parameters (e.g., surface roughness) were set as default values of the software. The hourly meteorological data (e.g., Ta, RH, Va, MRT) at 1.5m height above the ground were obtained through simulation. And the calculation of some thermal indices (e.g., PET, PMV, UTCI) was carried out by a particular module, "Biomet", in ENVI-met.

Table 1. Initial parameter values for the ENVI-met model simulation.

Data Type	Parameter	Input Value
Meteorological data	Initial temperature of atmosphere (°C)	26.4
	Relative humidity in 2 m (%)	80.5
	Specific humidity in 2500 m (g/kg)	8
	Wind speed (m/s)	1.1
	Wind direction (°)	135
	Microscale roughness length of surface (m)	0.01
Cloud setting	Low clouds	0
	Medium clouds	2
	High clouds	0
Soil data	Upper layer (0–20 cm) Ta (°C)	18
	Middle layer (20–50 cm) Ta (°C)	18
	Deep layer (50–100 cm) Ta (°C)	17
	Upper layer (0–20 cm) RH (%)	55
	Middle layer (20–50 cm) RH (%)	65

2.2.2. Model Validation

To verify the accuracy and reliability of the model in the microclimate simulation of small-scale parks, field weather condition measurement was implemented at four sample points (Figure 1b) on 28 June 2021. Four sample points were situated in different microenvironments: sample points 1 and 2 were in open squares and directly exposed to solar radiation; sample points 3 and 4 were encircled by abundant greenery and shaded by trees. This day was chosen for the field measurement since the weather was sunny, which was a relatively ideal condition to conduct the measurement during hot and humid summer. The Ta and RH were recorded by a HOBO meteorological station [34] in the solar radiation shield, while the global temperature and Va were collected by a Delta OHM HD [35] (Figure 1c). These instruments were placed at 1.5 m height from the ground same as in previous studies [33,36]. The logging interval was 1 min sampling, and continuous recording for 24 h was performed on the day of field weather condition measurement. Whereafter, the hourly average data were calculated for further analysis.

The Root Mean Square Error (RMSE) [37], the index of agreement (d) [38,39], and the coefficient of determination (R^2) [26] were adopted to evaluate the validity of the simulation results. Four receptors, corresponding to the actual sample points in the field measurements, have been designated within the model area. These receptors were selected for detailed monitoring of atmospheric processes, and the simulated Ta and RH at a height of 1.5m were extracted from these receptors. The RMSE (Equation (1)) and d (Equation (2)) were calculated through the following empirical algorithm. In general, if the d and R^2 tend to 1, while the RMSE tends to 0, the configuration of models was considered more accurate [26].

$$RMSE = \sqrt{\frac{\sum_{i=1}^{n}\left(X_i - X_i'\right)^2}{n}} \tag{1}$$

$$d = 1 - \frac{\sum_{i=1}^{n}\left(X_i' - X_i\right)^2}{\sum_{i=1}^{n}\left(|Y_i'| + |Y_i|\right)^2} \tag{2}$$

where, X_i denotes the measured value, X_i' denotes the simulated value, $Y_i' = X_i' - \overline{x}$, $Y_i = X_i - \overline{x}$, $\overline{x}$ denotes the average of the measured values.

As shown in Figure A1, the simulated and observed Ta and RH at four sample points for 24 h were compared by linear regression. The R^2 value for Ta is 0.92, and that for RH is 0.89, which are similar to or even better than the previous studies [30,40]. Furthermore, for Ta, the values of RMSE and the index d were 1.74 °C and 0.94, and for RH, the values were 2.16% and 0.95, respectively. As shown in Table A1, the R^2 of Ta and RH in the four sample

points ranges from 0.8–0.98, the RMSE of Ta and RH ranges from 0.67 °C–2.41 °C and 3.8%–7.01%, respectively, and the d-value is in the range of 0.95–0.98. In previous studies, the RMSE values vary from 0.26 to 4.30 °C for Ta and those for RH below 10.80% [27,41,42], and the values of the index d range from 0.60 to 0.93 [41]. Given that this study focuses on the relative value and trend of microclimatic fluctuation rather than an absolute quantity, the ENVI-met model under the aforementioned parameter setting can precisely recreate the microclimate conditions in the park.

2.3. Simulation Case Development Using Orthogonal Experiment Design

As an experimental design method, the orthogonal experiment design can select representative cases from full factorial experiments by means of a predefined orthogonality-based structural array, and thus efficiently reduce the number of studied cases and improve experimental efficiency [28]. Although the experimental runs are simplified, the orthogonal experiment design is equipped to yield a satisfactory factorial effect assessment and has been universally employed in the field of the built environment [27,43]. In an orthogonal experiment design, what causes the variation in experiment results is defined as an "element", while the distinct settings of the element are called a "level". Taguchi and Konishi [44] applied combinatorial mathematics theory to construct numerous standard orthogonal arrays. When conducting orthogonal experimental designs, one of the arrays can be directly utilized. The selection of an appropriate standard orthogonal array for a case study is dependent on the required degrees of freedom (f). When choosing an array, it is crucial to ensure that the number of rows not only meets or exceeds the necessary f, but also minimizes the number of experimental trials [45].

The TCC and three tree morphological elements, i.e., LAI, TH, and CD, were set as the elements in this orthogonal experiment design. As shown in Table 2, the levels of each element were listed as Level 1, Level 2, and Level 3 successively. The levels were determined based on the common range values of each element. The specific approach was to calculate the common range of a particular element, divide it into three equal intervals, and take the average value of each interval as the three levels of that element in the simulation experiment. Regarding TCC, we used the remote-sensing image to calculate the TCC of all urban parks within the Zhengzhou city area, totaling 124 parks, and found that the TCC of nearly three-quarters of parks ranges from 60% to 90%. According to the aforementioned method, in this study, the levels of TCC were determined to be 65%, 75%, and 85% successively. Furthermore, based on the tree morphology data obtained from a field survey in Lvyin Park, the levels of three tree morphological elements were calculated using the same method. Among them, the common range for TH was from 1.5 m to 4.5 m, and the levels were determined to be 2 m, 3 m, and 4 m. The common range for LAI was from 1.6 to 4.4, and the levels were determined to be 2.1, 3.0, and 3.9. The common range for CD was from 4 m to 10 m, and the levels were determined to be 5 m, 7 m, and 9 m. In ENVI-met's 3D plant editing tool (Albero), simulation-specific gridded tree modules can be generated by entering the appropriate combination of LAI, TH, and CD values [46], as shown in Figure 2. In ENVI-met, tree modeling needs the leaf area density (LAD) rather than LAI. Therefore, Equation (3) [40,47,48], which shows the relationship between LAD and LAI, was used to obtain the LAD of each height of the tree and consequently generate tree models with diverse CD and LAI. To avoid interference from quantitative factors, the other elements of the tree model, such as the albedo of leaves, and the depth of root and root area density, maintain the default settings.

$$LAI = \int_0^h LAD(z)dz \tag{3}$$

where LAI is the leaf area index, h is the total canopy height (m), $LAD(z)$ is the layer's leaf area density at height z (m^2/m^3), and dz is the layer's vertical size at height z (m).

In this study, we examined the impact of four elements (TCC, LAI, TH and CD) and the interactions among three tree morphological elements (LAI, TH, and CD). Each

element had three different levels. Theoretically, this would entail a total of 81 cases. However, to enhance experimental efficiency, we employed the orthogonal experiment method. In this method, f of each 3-level element is 2, and f of the interaction between two 3-level elements is 4 [45]. Consequently, the total required f can be calculated as follows: $2 \times 4 + 4 \times 3 = 20$. The standard orthogonal array L27, with 3 levels per column and 27 rows, was selected because it fulfills the requirements of f [45]. Based on this, 27 experimental protocol and simulation cases were developed (Table 3). This approach effectively reduced the number of trials by three-quarters. The level values of elements in each simulation case are located in the orthogonal table of L27, as shown in Table 3.

Table 2. Level values of each element used for orthogonal array assignment.

Element	Level 1	Level 2	Level 3
TH/m	2	3	4
LAI	2.1	3.0	3.9
CD/m	5	7	9
TCC/%	65	75	85

LAI: leaf area index, TH: trunk height, CD: crown diameter, TCC: tree canopy coverage.

Table 3. Simulation experimental protocol table.

Case Number	TH	LAI	CD	TCC
1	1	1	1	1
2	1	1	2	2
3	1	1	3	3
4	1	2	1	2
5	1	2	2	3
6	1	2	3	1
7	1	3	1	3
8	1	3	2	1
9	1	3	3	2
10	2	1	1	2
11	2	1	2	3
12	2	1	3	1
13	2	2	1	3
14	2	2	2	1
15	2	2	3	2
16	2	3	1	1
17	2	3	2	2
18	2	3	3	3
19	3	1	1	3
20	3	1	2	1
21	3	1	3	2
22	3	2	1	1
23	3	2	2	2
24	3	2	3	3
25	3	3	1	2
26	3	3	2	3
27	3	3	3	1

LAI_1 = 2.1, LAI_2 = 3.0, LAI_3 = 3.9, TH_1 = 2 m, TH_2 = 3 m, TH_3 = 4 m, CD_1 = 5 m, CD_2 = 7 m, CD_3 = 9 m, TCC_1 = 65%, TCC_2 = 75%, TCC_3 = 85%.
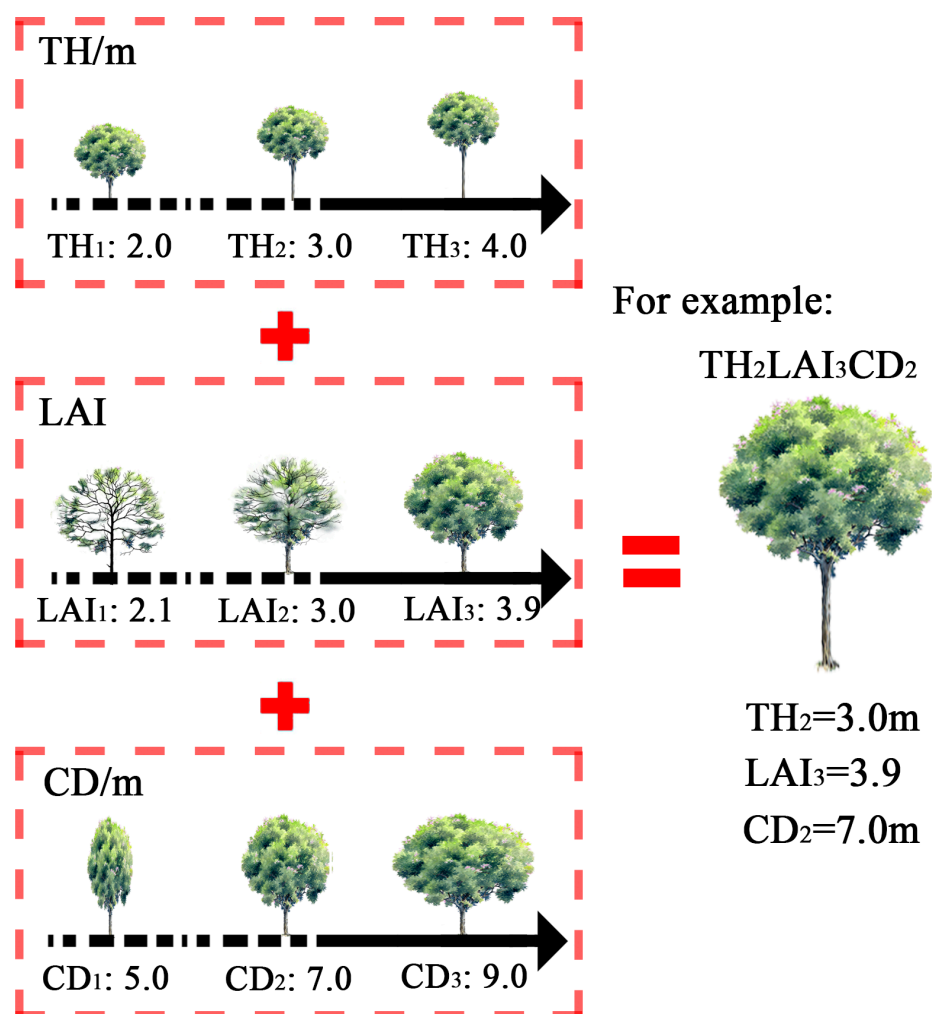
Figure 2. Levels of LAI, TH, and CD and tree example. Note on abbreviation—LAI: leaf area index, TH: trunk height, CD: crown diameter.

2.4. Thermal Comfort Index—PET

The PET thermal index was employed as the experimental indicator to evaluate thermal comfort for each simulation case. The index can be calculated within ENVI-met's post-processing tool, Biomet, by setting relevant human body parameters, such as age, gender, height, weight, static clothing insulation, and total metabolic rate, and combining them with the simulated meteorological output values, including Ta, RH, Va, and MRT [46]. PET was proposed by Höppe based on the Munich Energy-balance model for individuals (MEMI) and defined as Ta when the human heat exchange is balanced with the same skin and core temperature [49]. As the individual physiological features are taken into account when calculating the human thermal condition, PET was found to be more reliable and adopted to assess outdoor thermal comfort in related studies [32,50,51]. The configuration of the standardized personal parameters, as a reference for setting the human situation at the beginning of calculating PET, is as follows: male (gender), 1.75 m (height), 35 years old (age), 75 kg (weight), 0.9 clo (clothing thermal resistance), 80.21 W (activity metabolism), which is frequently adopted in previous works for ENVI-met simulation [40,52,53].

To precisely assess the human thermal perception for each simulation case, PET values can be divided into nine scales, each scale corresponding to a particular grade of thermal sensation (from "very cold" to "very hot") and physiological stress (from "extreme cold stress" to "extreme hot stress"). However, the range of PET values needs to be adjusted in accordance with local climatic conditions, as accomplished in some studies [54,55]. Mayer's team [17] issued questionnaires to obtain the intervals of PET values corresponding to

different thermal sensations and physiological stress in Munich (Table 4). This interval of PET values has been widely used in thermal comfort studies conducted in monsoon-influenced humid continental climate zones [56,57], and this study employed these PET intervals as the standard to assess the thermal comfort of each case, which has been utilized in other cities in the temperate continental climate zone of China [32,58].

Table 4. PET intervals correspond to different grades of thermal sensation and physiological stress.

PET (°C)	Thermal Sensation	Grade of Physiological Stress
<4	Very cold	Extreme cold stress
4–8	Cold	Strong cold stress
8–13	Cool	Moderate cold stress
13–18	Slightly cool	Slight cold stress
18–23	Neutral	No thermal stress
23–29	Slightly warm	Slight heat stress
29–35	Warm	Moderate heat stress
35–41	Hot	Strong heat stress
>41	Very Hot	Extreme heat stress

PET: physiological equivalent temperature (°C).

2.5. Statistical Analysis

Because the effects of TCC and morphological elements on the thermal environment in parks vary over time, it is important to comprehensively consider the temporal characteristics of users' activities when analyzing and evaluating park thermal comfort and discussing the optimal combination of elements. Existing research has confirmed that Chinese residents have higher activity frequencies in parks during the morning and evening, while the activity frequency is lower during the midday [59,60]. The more intense the activity, such as running, the more evident this characteristic becomes [59,60]. Generally, the number of users during the morning hours from 6:00 to 8:00 and the evening hours from 18:00 to 20:00 is approximately twice as much as during the midday hours from 12:00 to 14:00 [61,62]. In this study, we conducted a statistical analysis of simulated data for the high-frequency periods of activities among users, which include 6:00 to 8:00, 18:00 to 20:00, and the hottest period of the day at midday, from 12:00 to 14:00. The two most commonly used methods in the analysis of orthogonal experimental results, namely Range Analysis and Analysis of Variance (ANOVA), were employed to evaluate the impact of different greening elements on experimental indicator PET. In addition, taking into account the temporal characteristics of users' activities, the weights for the morning, midday, and evening are, respectively, set as 40%, 20%, and 40%. Then, the PET values for the morning, afternoon, and evening periods are weighted and averaged to determine the optimal combination of elements.

2.5.1. Range Analysis

Range analysis can reflect the extent of variation in the experimental indicator when the levels of elements change by calculating the *R*-value. The *R*-value represents the difference between the maximum and minimum values of the experimental indicator corresponding to different levels of the elements. A higher *R*-value indicates that the elements have a stronger impact on the experimental indicator, as calculated in Equations (4) and (5) [63]:

$$k_i = \frac{K_i}{s} \tag{4}$$

$$R = \max\{k_1, k_2, k_3 \dots\} - \min\{k_1, k_2, k_3 \dots\} \tag{5}$$

where k_i is the average of the experimental indicator at level i within a specific column (element) in the orthogonal experiments table (Table 3); K_i is the sum of experimental indicators at level i within the same column; s is the number of experiments indicators at level i.

2.5.2. Analysis of Variance

In this study, all statistical analyses concerning ANOVA were conducted using IBM SPSS Statistics 24. ANOVA is utilized to quantitatively assess the significance and magnitude of the effects of different elements and interactions between elements on experimental indicator PET. Before conducting ANOVA, it is necessary to test whether the experimental elements (TCC, TH, LAI, CD) are independent categorical variables, and we need to test the experimental data for normal distribution and homogeneity of variance [64]. To achieve this, we initially employed the Fisher's exact test, which is suitable for sample sizes less than 40, to examine the independence of the experimental elements. When the p-value exceeds 0.05, the categorical variables are considered to be independent at the significance level of 0.05 [65]. The p-values of our experimental elements, as determined by Fisher's exact test, were all 1, indicating that they meet the independence requirement at the significance level of 0.05. Secondly, since the ANOVA in this study specifically focused on examining the impact of the elements on the experimental indicator during three different time periods, separate tests for normal distribution and homogeneity of variance were conducted on the data from each time period to ensure the validity of the data analysis. When the p-value is greater than 0.05, it is considered that the experimental data follow a normal distribution and satisfies the assumption of homogeneity of variance at the significance level of 0.05 [64]. The results of our experimental data tests indicated that the p-values for normal distribution were 0.783 (morning), 0.394 (noon), and 0.667 (evening), while the p-values for homogeneity of variance were 0.895 (morning), 0.986 (noon), and 0.862 (evening), all of which were greater than 0.05. This indicated that the data conform to the requirements of normal distribution and homogeneity of variance at the significance level of 0.05.

On this basis, ANOVA is performed. The test report for the ANOVA typically includes several parameters, including error variance (f_e), degrees of freedom in column j (f_j), error sum of squares (s_e), F-value, and significance level (p). It should be noted that the F-value is directly proportional to the degree of influence of a single element or the interaction between elements, while p indicates a significant influence of the element or their interactions only if it is less than 0.05 [63].

Furthermore, the contribution ratio (ρ_j/%) (Equation (9)) [66,67] can be used to quantify the proportion of influence of each element or interaction between elements on the experimental indicator PET. It is collectively determined by the sum of squared column deviations (Equations (6) and (7)) [66–68], the sum of squared total deviations (Equation (8)) [66,69] and other parameters including f_e, s_e, and f_j. The higher ρ_j is, the greater the influence of the element or interaction between elements on the experimental indicator PET.

$$S_j = \frac{b}{a}\sum\nolimits_{k=1}^{b} y_{jk}^2 - \frac{1}{a}\left(\sum\nolimits_{i=1}^{a} y_i\right)^2 \tag{6}$$

$$\sum\nolimits_{k=1}^{3} y_{jk}^2 = K_1^2 + K_2^2 + K_3^2 \tag{7}$$

$$S = \sum\nolimits_{i=1}^{a} (y_i - \overline{y})^2 \tag{8}$$

$$\rho_j = \frac{S_j - \frac{s_e}{f_e} f_j}{S} \times 100\% \tag{9}$$

where S_j is the sum of squared column deviations; S is the sum of squared total deviations; a is the total number of experiments; b is the total number of levels; j is the column number; i is the experimental case number; k is the level number; y_i is the experimental indicator PET; $K_{1,2,3}$ is the sum of the PET of the cases in which the level of the element (i.e., TH, LAI, CD and TCC) is, respectively, 1, 2, and 3.

3. Results

3.1. The Difference in Thermal Comfort of Studied Cases

3.1.1. PET Variation during Different Periods

Initially, the analysis of PET variation within the park was performed to understand how the thermal environment of the studied cases changes within a day (Figure 3). Between 7:00 and 18:00, due to the influence of solar radiation, there are significant changes in the thermal environment within the park. PET fluctuates greatly, ranging from 25.3 °C to 43.0 °C. During this time, the extreme thermal sensation of "Very hot" appears, and the maximum difference in PET values is 8.94 °C among the 27 studied cases. In addition, the thermal environment did not change significantly during other periods not influenced by solar radiation, their PET values range between 22.1 °C and 27.5 °C, and the thermal sensation levels fall between "slightly cool" and "neutral".

Table 5 presents the differences in PET values among the 27 studied cases at various times of the day, of which the gradient indicates the ratio of the difference between the maximum and minimum PET values (ΔPET) to the maximum value. In Table 5, the ΔPET from 7:00 to 18:00 was significantly higher than the other time periods, suggesting that PET could be significantly reduced between 7:00 and 18:00 by altering the canopy cover and tree morphology characteristics. During this period, the PET gradient is consistently above 10%, with the highest PET gradient appearing at 10:00 and 17:00 (21.35% and 21.44%). For most of the other periods, the gradient is between 2% and 5%.
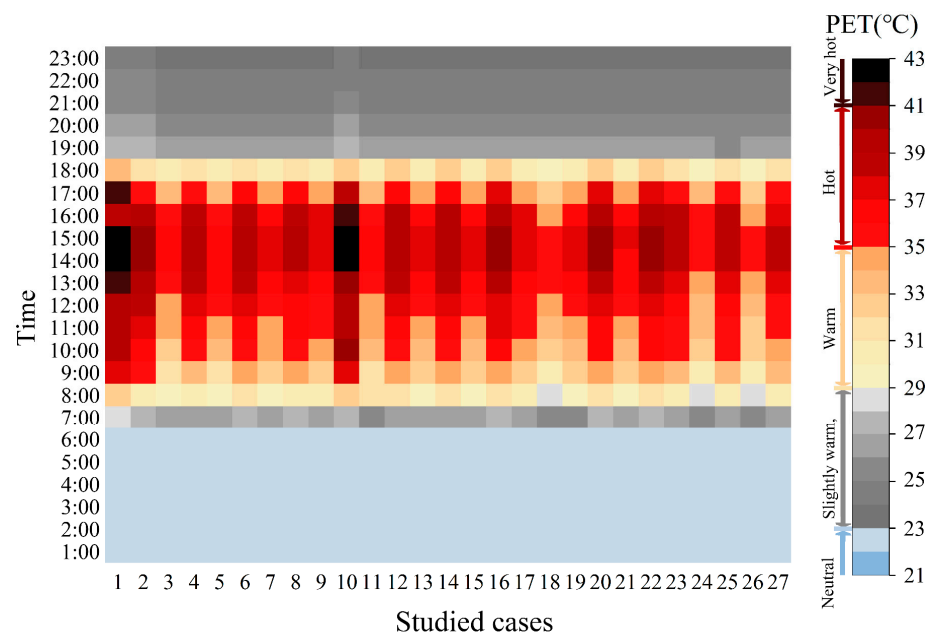
Figure 3. PET heatmap of 27 study cases throughout the day.

Table 5. The hourly value of Max PET, Min PET, ΔPET, gradient throughout the day.

Time (h)	Max PET (°C)	Min PET (°C)	ΔPET (°C)	Gradient (%)
1:00	22.87	22.32	0.55	2.40
2:00	22.82	22.23	0.59	2.59
3:00	22.78	22.16	0.62	2.72
4:00	22.73	22.09	0.64	2.82
5:00	22.87	22.22	0.65	2.84
6:00	22.85	22.17	0.68	2.98
7:00	28.39	25.31	3.08	10.85
8:00	32.81	28.30	4.51	13.75
9:00	37.29	30.88	6.41	17.19
10:00	40.89	32.16	8.73	21.35
11:00	39.66	32.94	6.72	16.94

Table 5. *Cont.*

Time (h)	Max PET (°C)	Min PET (°C)	ΔPET (°C)	Gradient (%)
12:00	39.87	33.83	6.04	15.15
13:00	41.14	34.86	6.28	15.26
14:00	42.80	35.50	7.30	17.06
15:00	43.01	35.42	7.59	17.65
16:00	41.53	34.91	6.62	15.94
17:00	41.70	32.76	8.94	21.44
18:00	33.39	29.65	3.74	11.20
19:00	27.50	25.5	1.93	7.02
20:00	26.28	25.11	1.17	4.45
21:00	25.36	24.32	1.04	4.10
22:00	25.02	24.03	0.99	3.96
23:00	24.30	23.45	0.85	3.50

Max PET: maximum of physiological equivalent temperature; Min PET: minimum of physiological equivalent temperature; ΔPET: difference between Max PET and Min PET; Gradient: the ratio of ΔPET to the maximum of physiological equivalent temperature.

3.1.2. Thermal Sensation Levels in Different Studied Cases

Figure 4 shows the proportion of different thermal sensation levels in each studied case throughout the entire day. It is evident that Cases 1 and Case 10, with most levels of the four elements being 1 or 2, have relatively poor thermal comfort, as they both experience the "Very hot" sensation level, accounting for 17% and 13%, respectively. Conversely, Cases 3, 11, 18, 24, and 26 demonstrate relatively good thermal comfort, with the highest thermal sensation level being "Hot", accounting for less than 20%. Among these cases, Case 26, with most levels of the four elements being 3, has the lowest percentage of "Hot" sensation, at just 9%, signifying the highest level of comfort.
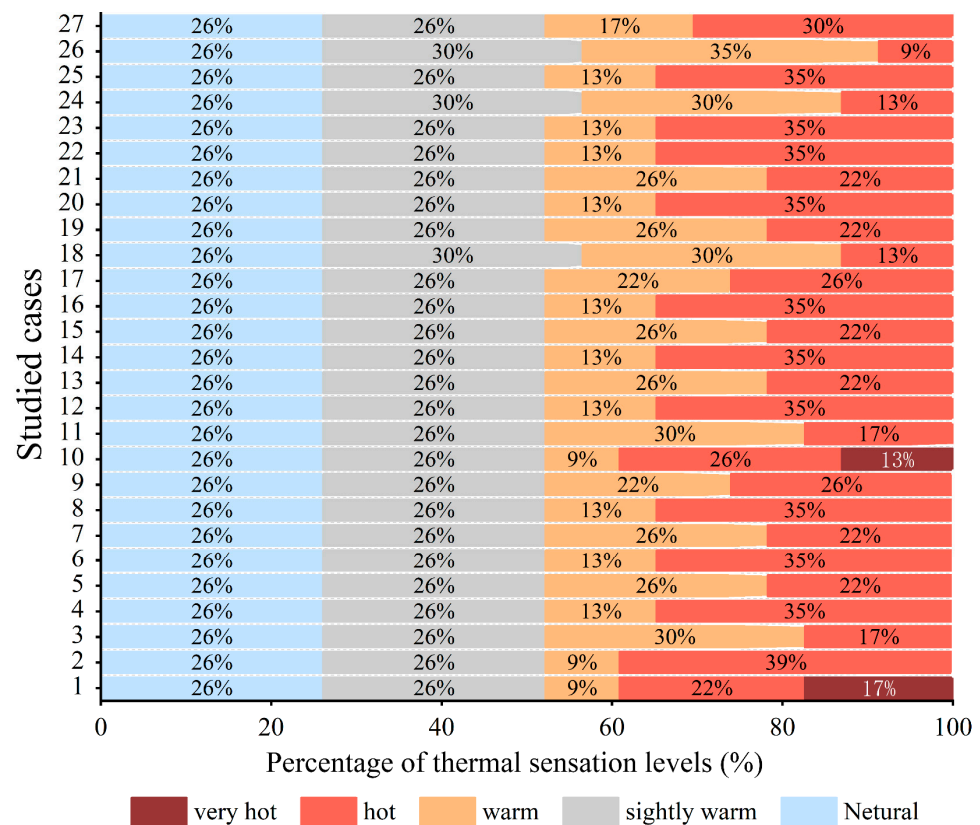

Figure 4. Percentage of thermal sensation levels throughout the day for 27 studied cases. Refer to Table 4 for thermal sensation level classification criteria.

3.2. Effect of TCC on PET

As shown in Figure 5, there is a downward trend in PET as the TCC increases continuously from 65% to 85%. It can be observed that as TCC increases, the average daily PET decreases by 1.51 °C. This indicates that TCC has the potential to improve the thermal comfort of the park. In addition, the R-value was able to reflect the differences in efficiency of TCC's impact on PET at different periods of the day. The R-value rankings for each time period are as follows: midday (2.97 °C) > morning (1.16 °C) > evening (1.01 °C). This shows that TCC has the greatest effect on PET at midday, with an R-value approximately 2.5–3 times higher than in the morning and evening.
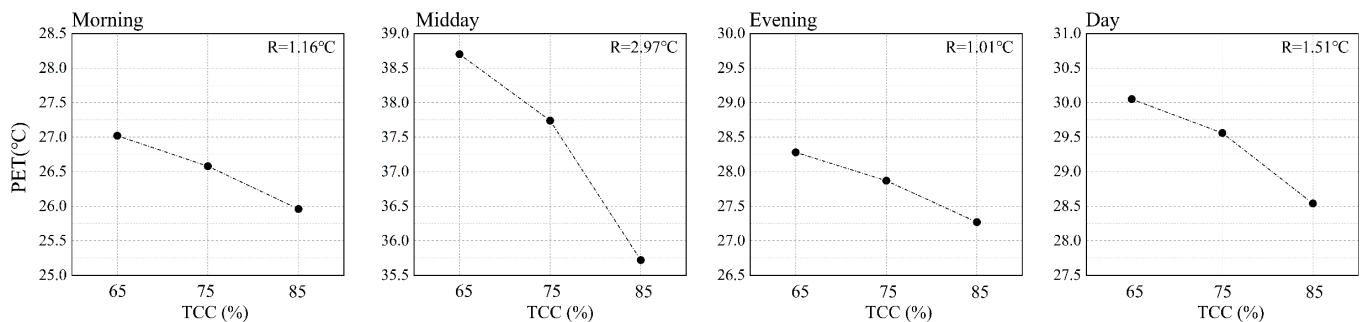
Figure 5. Changes in average PET values for three TCC levels: morning (6:00–8:00), midday (12:00–14:00), evening (18:00–20:00), and the whole day (0:00–23:00).

Furthermore, as the TCC in the park increases, the magnitude of the decline in PET becomes significantly larger. When TCC increases from 65% to 75%, the decrease in the daily average PET is only 1.6%. However, when TCC increases from 75% to 85%, the decrease in the daily average PET more than doubles to 3.4%. This phenomenon is equally pronounced during the midday period. The difference in PET values between a TCC of 65% and 75% is 0.96 °C, while the difference between a TCC of 75% and 85% increases to 2.02 °C.

In summary, the higher the tree canopy cover, the greater the extent of improvement in the thermal environment. When the tree canopy cover exceeds 75%, the cooling effect becomes even more pronounced.

3.3. Effect of Morphological Elements of Trees on PET
3.3.1. Effect of TH on PET

Figure 6 shows a decreasing trend in PET as TH increases continuously from 2m to 4m. However, the magnitude of the decline only slightly varies. Specifically, an increase in TH from 2 m to 3 m corresponds to a decrease of approximately 0.8% in daily average PET, while an increase from 3 m to 4 m results in a decrease of around 1.1%.
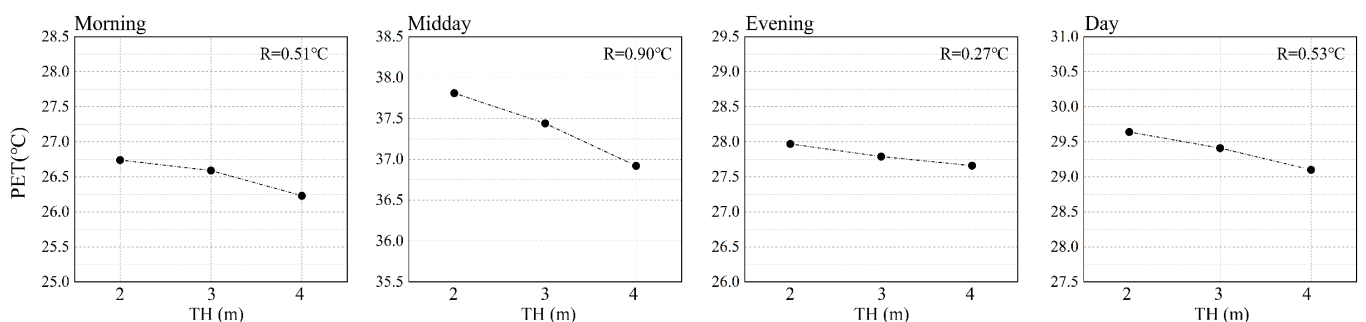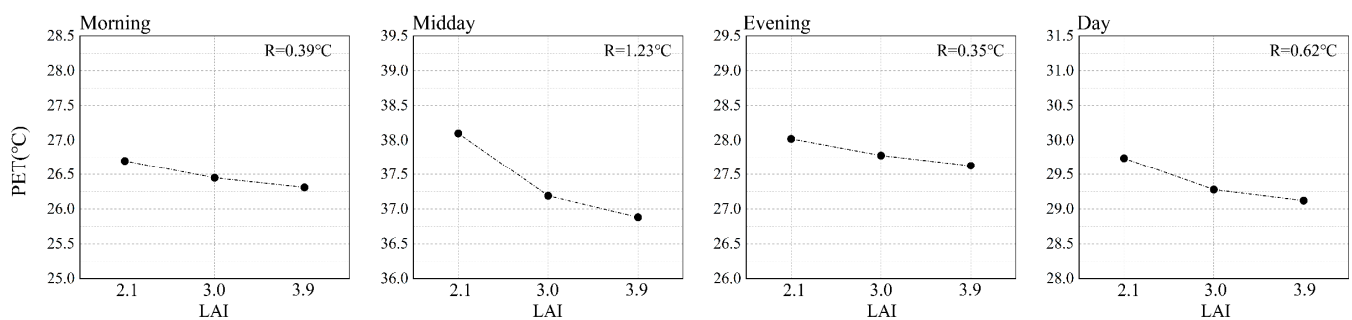

Figure 6. Changes in average PET values for three TH levels: morning (6:00–8:00), midday (12:00–14:00), evening (18:00–20:00), and the whole day (0:00–23:00).

The influence of TH on PET varies across different periods of the day. The R-value rankings for each time period are as follows: midday (0.90 °C) > morning (0.51° C) > evening (0.27 °C). It is observed that the R-values throughout the day do not exceed 1 °C, indicating that this element has a relatively small impact on PET compared to TCC.

3.3.2. Effect of LAI on PET

As shown in Figure 7, there is a downward trend in PET as the LAI increases continuously from 2.1 to 3.9. It is worth noting that a higher LAI is not necessarily better. Based on the daily average PET, when the LAI increases from 2.1 to 3.0, there is a 1.5% decrease in PET, while the increase from 3.0 to 3.9 only results in a 0.6% change in PET. This indicates that while increasing LAI can enlarge the shaded area and reduce ground heat, at the same time, excessive foliage density can also inhibit air circulation, potentially diminishing the efficiency of trees in improving thermal comfort.
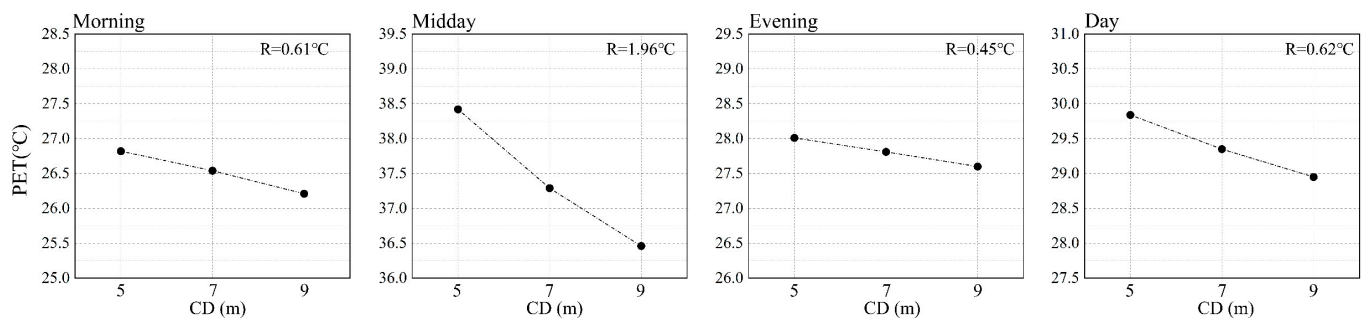

Figure 7. Changes in average PET values for three LAI levels: morning (6:00–8:00), midday (12:00–14:00), evening (18:00–20:00), and the whole day (0:00–23:00).

In the morning and evening, LAI has a smaller and more or less the same effect on PET, but the effect is visible in the midday, as shown in Figure 7. The R-value rankings for each time period are as follows: midday (1.23 °C) > morning (0.39 °C) > evening (0.35 °C). This difference is primarily due to the radiation variations between the periods.

3.3.3. Effect of CD on PET

The variation trend between CD and PET is similar to that of the LAI (Figure 8). PET exhibits a consistent decline as CD gradually rises from 5 m to 9 m, and as the CD increases, the magnitude of the decrease in PET becomes smaller. When the CD increases from 5 m to 7 m, the daily average PET reduction is approximately 1.7%. When the CD increases from 7 m to 9 m, the daily average PET reduction is approximately 1.4%. This indicates that increasing the CD of a tree, while enhancing shading effects, may also hinder air circulation.

Figure 8. Changes in average PET values for three CD levels: morning (6:00–8:00), midday (12:00–14:00), evening (18:00–20:00), and the whole day (0:00–23:00).

Figure 8 shows that altering the CD has a more visible impact on improving the thermal environment during the midday when solar radiation is stronger, compared to the

morning and evening. The R-value rankings for each time period are as follows: midday (1.96 °C) > morning (0.61 °C) > evening (0.45 °C). This is primarily because the CD directly determines the shading area.

3.4. Comparison of the Impact of the Elements

3.4.1. Comparison of Different Levels of the Elements

By comparing the PET differences (ΔPET) between adjacent levels of each greening element (Figure 9), we analyzed the importance of each element on PET and the differences in the impact between the different levels of each element. Overall, we observed temporal differences in the regulation of PET by each element. The largest ΔPET was observed during the midday period, while the morning and evening periods showed relatively smaller changes. This suggests that changing the level of greening elements has a stronger impact on regulating the thermal environment during midday, but a relatively weaker effect during the morning and evening periods.
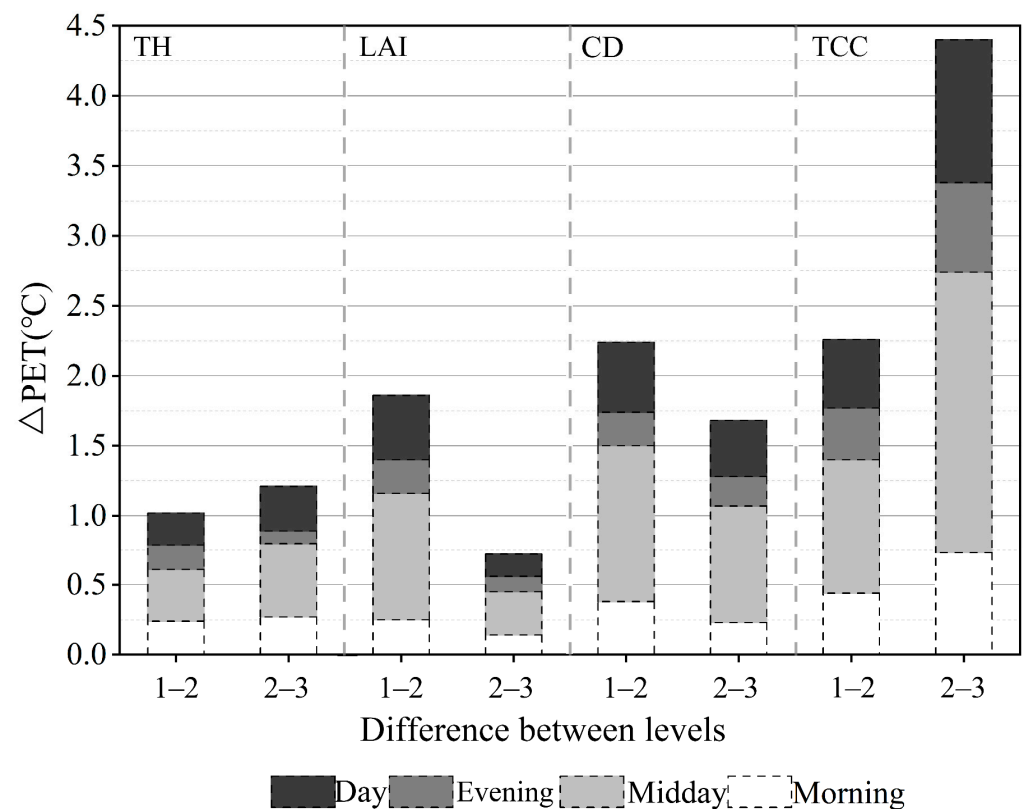
Figure 9. ΔPET between adjacent levels of each greening element during morning (6:00–8:00), midday (12:00–14:00), evening (18:00–20:00), and the whole day (0:00–23:00). Note on abbreviation—ΔPET: difference of physiological equivalent temperature.

Considering the average daily ΔPET values of adjacent levels for each element, the change in TCC has the largest impact on ΔPET, followed by CD, while LAI and TH have relatively smaller effects. The ΔPET values between the different levels of TH are similar, while for LAI and CD, the ΔPET between level 1 and level 2 is greater than the ΔPET between level 2 and level 3. Additionally, the ΔPET between level 2 and level 3 for TCC is greater than the ΔPET between level 1 and level 2. This indicates that higher levels of the four greening elements result in more effective improvement in thermal comfort within the park. Specifically, within the range of 2.1 to 3.0 for LAI, 5–7 m for CD, and above 75% for TCC, there is a higher efficiency in improving thermal comfort in the park.

3.4.2. Comparing the Contribution of Each Element on PET

Further ANOVA analysis is conducted to assess the extent and significance of each element's influence on the park's thermal environment (Table 6). The results indicate that the *p*-values for TH, LAI, CD, and TCC are all below 0.05 during the morning, midday, and evening periods, signifying a significant impact on park PET. However, the *p*-values for the interaction effects between any two of the three morphological elements are all above 0.05, indicating that the interaction between these elements does not have a significant impact on PET in the park. According to the F-values, during the morning period, the elements are ranked in terms of their importance as follows: TCC > CD > TH > LAI. During the noon and evening periods, the elements are consistently ranked in terms of their importance as follows: TCC > CD > LAI > TH.

Table 6. ANOVA results for the effects of each element and their interactions at different periods.

Elements & Combinations	Morning		Midday		Evening	
	F	P	F	P	F	P
TH	17.23	0.00	6.27	0.03	12.27	0.01
LAI	10.28	0.01	12.56	0.01	20.84	0.00
CD	24.94	0.00	29.85	0.00	32.71	0.00
TCC	90.62	0.00	71.17	0.00	168.44	0.00
TH × LAI	1.33	0.36	1.87	0.23	3.12	0.10
TH × CD	1.34	0.36	1.12	0.43	0.79	0.57
LAI × CD	1.39	0.34	1.90	0.23	2.49	0.15

$p > 0.05$: not significant, $p < 0.05$: significant.

Based on this, the contribution ratio of each element to PET is calculated using Equations (3)–(6) to quantify their importance in influencing thermal comfort. As indicated in Figure 10, each element plays a distinctive role during different periods. Overall, TCC had the greatest contribution, followed by CD. LAI and TH made similar contributions, albeit to a lesser extent. Specifically, the contribution ratio of TCC during each period exceeds 50%, which is higher than the sum of the contribution ratios of the other three tree morphological elements. The contribution ratio of TCC shows a decreasing-then-increasing trend over time, with the highest contribution ratio during the evening period at 67%. Among the three plant morphological elements, CD has the largest contribution. Its contribution ratio shows an increasing-then-decreasing trend over time, reaching a peak during the midday period, close to 22%. TH has a relatively high contribution ratio of over 10% in the morning, but less than 5% in other periods. The contribution ratio of LAI shows minor differences across different periods, with a slightly higher contribution ratio during the midday period, close to 9%.

3.5. Optimization of Park Trees

Based on the time weights allocated in Section 2.5, the PET values for the morning, midday, and evening periods are weighted and averaged to determine the optimal combination of elements (Figure 11). Case 26, which consists of a combination of 85% TCC, 4 m TH, 3.9 LAI, and 7m CD, is identified as the optimal research case. This case has the lowest weighted average PET value of 27.9 °C.

Previous research has shown that when the PET value does not exceed 29 °C, the thermal sensation experienced by the human body does not exceed a slightly warm level [20]. Considering that the slightly warm outdoor thermal environment in summer is still acceptable to the human body, the standard for achieving thermal comfort in summer parks is set with a PET value not exceeding 29 °C. According to Figure 11, it can be inferred that there are 13 cases in the simulation cases that meet the thermal comfort requirements for parks in summer. Among them, there are four cases with 75% TCC and nine cases with 85% TCC. It can be observed that all the cases with an 85% TCC meet the comfort requirements, thus providing more flexibility in selecting the levels of the other three elements. However, for

the case with a 75% TCC to meet the thermal comfort requirements during summer, it is necessary to select and plant trees with a canopy size of at least 7 m. Moreover, when the CDs are at the same level, the case with taller tree trunks provides better thermal comfort. On the other hand, there is no clear pattern for selecting the level of LAI in the optimization scheme. Instead, a reasonable LAI needs to be determined based on TCC, CD, and TH.
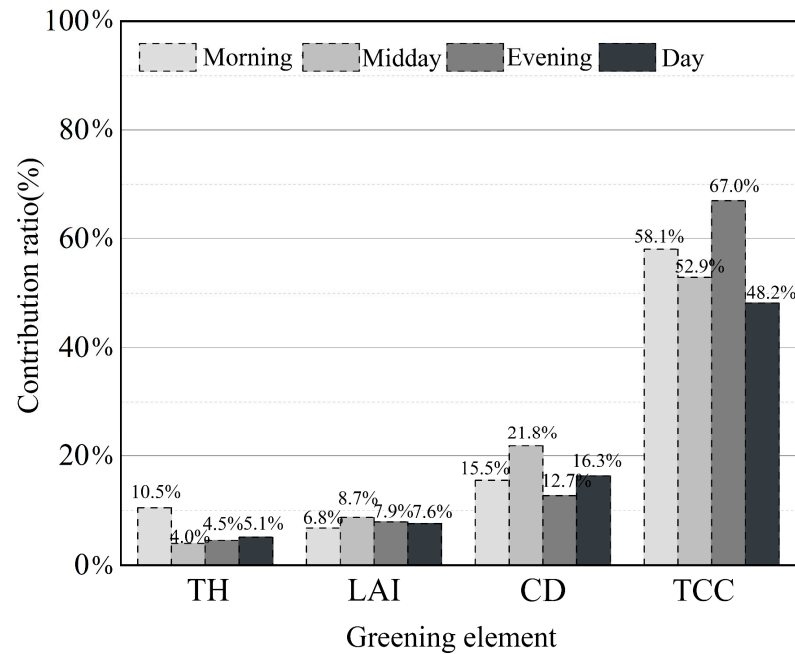

Figure 10. Contribution ratio of each element during morning (6:00–8:00), midday (12:00–14:00), evening (18:00–20:00), and the whole day (0:00–23:00).
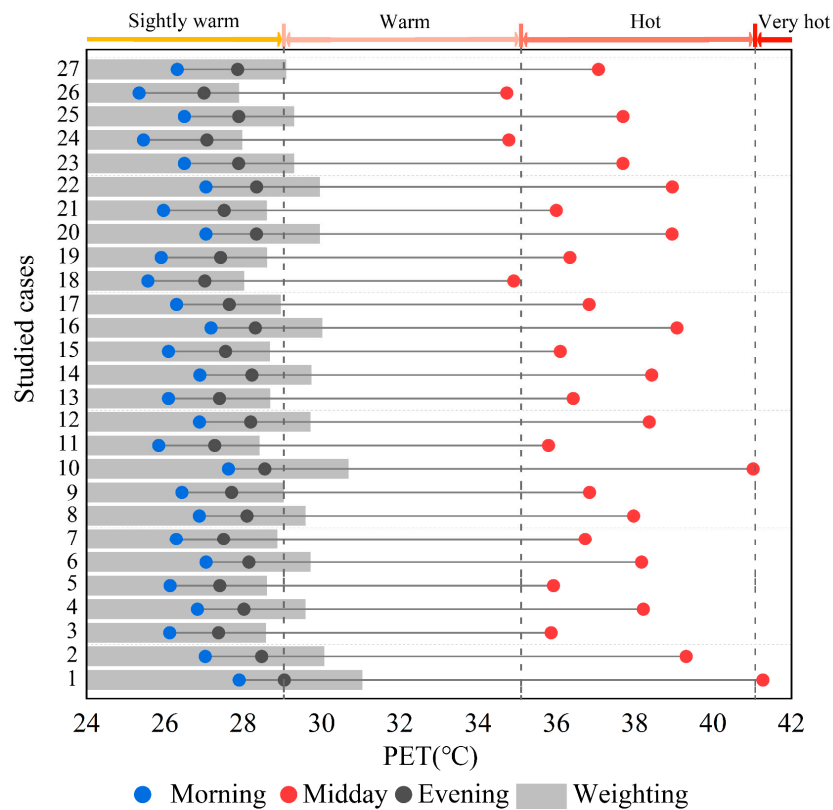

Figure 11. PET and weighted average for each studied case during morning (6:00–8:00), midday (12:00–14:00), evening (18:00–20:00).

4. Discussion

Urban forests have a significant cooling effect, and trees are one of the important elements in mitigating heat [21,25]. Tree coverage and morphology have an impact on the cooling effect and outdoor thermal comfort [23,53,70], a phenomenon that has been widely studied and demonstrated in different regions. In this study, we utilized orthogonal experimental design and simulation modeling techniques to quantitatively analyze the effects of tree coverage and morphological elements, namely, TH, LAI, and CD, on thermal comfort in the park during summer. Additionally, the present study fills the research gap in the existing studies regarding the temporal differences in the effects of various elements (TCC, LAI, TH, and CD) on thermal comfort.

The results indicate that TCC is the most significant element observed to affect thermal comfort. It is similar to the findings of Li et al. [71], who quantitatively studied the impact of different greening elements on thermal comfort in urban street canyons and found that changes in tree planting density had the greatest impact on the thermal environment while increasing the LAI had limited benefits. This may be due to the influence of multiple meteorological elements such as wind speed and solar radiation on thermal comfort [17]. A higher LAI can not only enhance transpiration and shading effects, but also impede air movement, thereby affecting the effectiveness of LAI in improving thermal comfort. Our findings also differ from some studies, such as the research conducted by Morakinyo et al. [40], which explored the importance ranking of tree morphological elements on the thermal benefits. They found that when the TCC is 30%, the LAI is the most significant influencing element, followed by TH, tree height, and CD. However, their study only investigated the role of tree morphological elements under specific TCC in high-density urban areas, which may affect the thermal benefits of plants due to the shade cast by surrounding tall buildings. Trees located in the shadows of buildings have a weaker cooling effect compared to those exposed to solar radiation [23]. Additionally, the TCC in their study is only 30%, much lower than that in our study (TCC ranging from 65% to 85%). This indicates that variations in TCC can potentially affect the importance of various tree morphological elements in improving the thermal environment. The results also indicate that TH is the weakest element observed to affect thermal comfort. Nevertheless, increasing TH can still to some extent improve summer thermal comfort, but its impact on thermal comfort may vary at different times. This may be related to solar radiation, as the height variation of tree trunks can potentially impact the effect of tress shade. Additionally, it is worth mentioning that the impact efficiency of changes in elemental levels on thermal comfort is not constant, especially at midday. This is often due to the combined effects of solar radiation and wind [26]. Therefore, when considering the crown coverage and morphological characteristics of trees, it is necessary to balance their shading effects and wind-blocking impacts [72].

Furthermore, we also observed that the contribution ratios of different tree morphological elements to thermal comfort vary depending on the time of day. In the morning, the contribution ratio of TH is higher than that of LAI, while during midday and evening, the situation is exactly the opposite. This may be owing to the close relationship between LAI and solar radiation, while TH primarily affects ventilation [71]. In the morning, the solar altitude is low, and solar radiation is weak, resulting in a relatively greater impact of the ventilation and cooling effect provided by TH on thermal comfort [40]. During midday, when the solar altitude is high and solar radiation is strong, the most direct way to alleviate thermal discomfort is by shading the solar radiation, and LAI is an important element for the shading benefits of trees [73]. In the evening, although there is no solar radiation, LAI, the importance of which is slightly higher than TH, directly affects the surface heat dissipation. Therefore, it is necessary to select suitable tree species based on the meteorological characteristics at various times throughout the day [74].

However, due to the limited number of simulated cases and time constraints in this study, there are certain limitations to the research results. To be specific, wind speed has a huge impact on outdoor thermal comfort, but due to the limitation of ENVI-met,

only a constant wind speed was set in this study [26]. It is not yet known whether the influence of the elements studied on outdoor thermal comfort is valid or not with the change in wind speed. Moreover, the standardized personal parameters were applied in the calculation of PET. Since personal characteristics, such as age, sex, and active metabolic rate, also affect the perception of outdoor thermal comfort, interpersonal differences should be taken into account in further studies. The numerical simulation scheme in this study was developed through orthogonal experiment design, the greatest advantage of which lies in reducing the number of simulation scenarios and improving the experimental efficiency. The amount of impact elements and their levels are subject to the fixed format of the selected orthogonal table, making it difficult to clarify the quantitative relationship between additional elements and the microclimate in the park. It is also necessary to explore the impact of other elements on the microclimate in the park, such as the arranging method of trees and the ratio of the combination of trees, shrubs, and grasses. Further study needs to be conducted to quantify the correlation between trees' morphological elements and thermal comfort indices and examine whether it is a linear or nonlinear regression relationship. Identifying the correct type of relationship is crucial for developing an accurate and reliable model. On one hand, this helps researchers to more accurately describe the relationship between urban greening and thermal comfort and gain a deeper understanding of the underlying mechanisms and processes involved. On the other hand, this facilitates in-depth exploration of the efficiency and thresholds of urban greening in improving thermal comfort, enabling more reliable predictions of urban green spaces' thermal comfort. This enhances the effectiveness of urban landscape planning and design interventions related to thermal comfort [33]. The study results are based solely on data analysis from a single date, whereas parks are used differently throughout the year. For instance, during the summer, people tend to engage in activities primarily during the cooler early morning and evening hours, whereas in winter, they might prefer warmer midday activities. Additionally, the regulation of trees on outdoor thermal comfort varies significantly with different seasons. For example, evergreen trees can improve outdoor thermal comfort in summer by shading solar radiation, while this effect may reduce the thermal comfort experience during winter. Therefore, a longer-term and full-season experiment should be conducted in the future to help capture the seasonal variations in season, time, and park usage, and to provide a more holistic understanding of the impact of trees on thermal comfort. Besides the direct cooling effect through shading and transpiration, trees can also indirectly impact building energy consumption by altering the microclimate in the three-dimensional space around the building and building surface temperature. Further studies can explore the relationship between the morphological characteristics of trees and building energy consumption, thereby providing guidance on tree selection and layout for decision-makers and designers from the energy-saving perspective.

5. Conclusions

The study's findings reveal that TCC and tree morphological elements, including LAI, TH, and CD, all have the potential to improve outdoor thermal comfort during the summer, particularly during the midday period when their impact is most pronounced. While these greening elements display variations in their effects on the park's thermal environment during the morning, midday, and evening, TCC consistently emerges as the most influential element in improving outdoor thermal comfort during the summer. Its contribution surpasses the combined effect of the other three tree morphological elements. Specifically, during the evening, TCC contributes up to 67% of the impact on PET among all the studied elements. Among the three tree morphological elements, LAI, CD, and TH, TH exhibits a relatively higher influence on PET during the morning, while LAI and CD show a relatively stronger impact on PET during midday. Furthermore, when evaluating various combinations of these elements, it was determined that a configuration consisting of 85% TCC, 4 m TH, 3.9 LAI, and 7 m CD provided the most comfortable summer thermal environment for the park.

Based on the research, given a certain TCC, the tree species should be reasonably chosen in accordance with the morphological characteristics and the spatial usage requirements during different periods so as to balance shading and ventilation. Through optimizing the configuration of trees, the microclimate in the park during summer can be effectively improved, which is conducive to creating comfortable and healthy activity places for residents, enhancing their enthusiasm and participation in fitness, and increasing the frequency of outdoor activities.

Author Contributions: Conceptualization, S.X., X.C. and K.W.; methodology, X.C. and J.W.; software, J.W.; validation, X.C., Y.M. and M.L.; formal analysis, K.W. and J.W.; investigation, S.X. and X.C.; resources, K.W.; data curation, S.X. and J.W.; writing—original draft preparation, S.X. and X.C.; writing—review and editing, S.X., X.C. and K.W.; visualization, K.W., X.C. and J.X.; supervision, S.X.; project administration, S.X.; funding acquisition, S.X. and K.W. All authors have read and agreed to the published version of the manuscript.
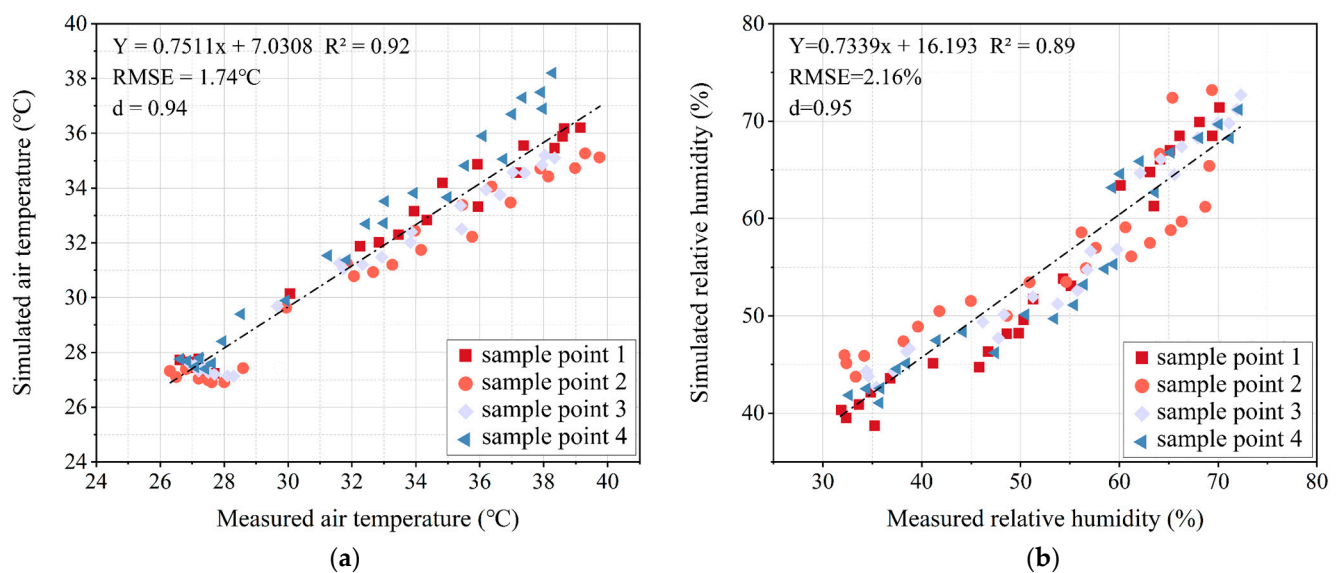
Data Availability Statement: No new data were created, and data are unavailable due to privacy or ethical restrictions.

Conflicts of Interest: The authors declare no conflict of interest.

Appendix A

Figure A1. Linear fitting between the simulated and measured data: (**a**) air temperature; (**b**) humidity. Note on abbreviation—RMSE: root mean square error; d: index of agreement.

Table A1. Linear regression equations, R^2, RMSE and d-value for measured and simulated data at each sample point.

Sample Points	Ta			RH		
	Equation	RMSE (°C)	d	Equation	RMSE (%)	d
1	y = 0.7458x + 7.344 $R^2 = 0.96$	1.54	0.98	y = 0.7458x + 7.344 $R^2 = 0.98$	3.80	0.98
2	y =0.6746x + 8.819 $R^2 = 0.96$	2.41	0.97	y = 0.5642x + 25.741 $R^2 = 0.81$	7.01	0.95
3	y = 0.7283x + 7.392 $R^2 = 0.97$	1.88	0.96	y = 0.7585x + 15.124 $R^2 = 0.94$	4.42	0.98
4	y = 0.8876x + 3.573 $R^2 = 0.98$	0.67	0.98	y = 0.7633x + 14.276 $R^2 = 0.91$	4.60	0.97

RMSE: root mean square error; d: index of agreement.

References

1. Senanayake, I.P.; Welivitiya, W.D.D.P.; Nadeeka, P.M. Remote Sensing Based Analysis of Urban Heat Islands with Vegetation Cover in Colombo City, Sri Lanka Using Landsat-7 ETM+ Data. *Urban Clim.* **2013**, *5*, 19–35. [CrossRef]
2. Kolokotroni, M.; Giridharan, R. Urban Heat Island Intensity in London: An Investigation of the Impact of Physical Characteristics on Changes in Outdoor Air Temperature during Summer. *Sol. Energy* **2008**, *82*, 986–998. [CrossRef]
3. Min, M.; Zhao, H.; Miao, C. Spatio-Temporal Evolution Analysis of the Urban Heat Island: A Case Study of Zhengzhou City, China. *Sustainability* **2018**, *10*, 1992. [CrossRef]
4. García-Herrera, R.; Díaz, J.; Trigo, R.M.; Luterbacher, J.; Fischer, E.M. A Review of the European Summer Heat Wave of 2003. *Crit. Rev. Environ. Sci. Technol.* **2010**, *40*, 267–306. [CrossRef]
5. Luber, G.; McGeehin, M. Climate Change and Extreme Heat Events. *Am. J. Prev. Med.* **2008**, *35*, 429–435. [CrossRef] [PubMed]
6. Sun, S.; Xu, X.; Lao, Z.; Liu, W.; Li, Z.; Higueras García, E.; He, L.; Zhu, J. Evaluating the Impact of Urban Green Space and Landscape Design Parameters on Thermal Comfort in Hot Summer by Numerical Simulation. *Build. Environ.* **2017**, *123*, 277–288. [CrossRef]
7. Zheng, S. Experimental and Theoretical Study of Urban Tree Instantaneous and Hourly Transpiration Rates and Their Cooling Effect in Hot and Humid Area. *Sustain. Cities Soc.* **2021**, *68*, 102808. [CrossRef]
8. Chen, L.; Wen, Y.; Zhang, L.; Xiang, W.-N. Studies of Thermal Comfort and Space Use in an Urban Park Square in Cool and Cold Seasons in Shanghai. *Build. Environ.* **2015**, *94*, 644–653. [CrossRef]
9. Jo, H.-K.; Kim, J.-Y.; Park, H.-M. Carbon Reduction and Planning Strategies for Urban Parks in Seoul. *Urban For. Urban Green.* **2019**, *41*, 48–54. [CrossRef]
10. Xu, M.; Hong, B.; Mi, J.; Yan, S. Outdoor Thermal Comfort in an Urban Park during Winter in Cold Regions of China. *Sustain. Cities Soc.* **2018**, *43*, 208–220. [CrossRef]
11. Yan, H.; Wu, F.; Dong, L. Influence of a Large Urban Park on the Local Urban Thermal Environment. *Sci. Total Environ.* **2018**, *622–623*, 882–891. [CrossRef] [PubMed]
12. Seto, K.C.; Güneralp, B.; Hutyra, L.R. Global Forecasts of Urban Expansion to 2030 and Direct Impacts on Biodiversity and Carbon Pools. *Proc. Natl. Acad. Sci. USA* **2012**, *109*, 16083–16088. [CrossRef] [PubMed]
13. Marando, F.; Heris, M.P.; Zulian, G.; Udías, A.; Mentaschi, L.; Chrysoulakis, N.; Parastatidis, D.; Maes, J. Urban Heat Island Mitigation by Green Infrastructure in European Functional Urban Areas. *Sustain. Cities Soc.* **2022**, *77*, 103564. [CrossRef]
14. Sodoudi, S.; Zhang, H.; Chi, X.; Müller, F.; Li, H. The Influence of Spatial Configuration of Green Areas on Microclimate and Thermal Comfort. *Urban For. Urban Green.* **2018**, *34*, 85–96. [CrossRef]
15. Liu, Z.; Brown, R.D.; Zheng, S.; Jiang, Y.; Zhao, L. An In-Depth Analysis of the Effect of Trees on Human Energy Fluxes. *Urban For. Urban Green.* **2020**, *50*, 126646. [CrossRef]
16. Karimi, A.; Sanaieian, H.; Farhadi, H.; Norouzian-Maleki, S. Evaluation of the Thermal Indices and Thermal Comfort Improvement by Different Vegetation Species and Materials in a Medium-Sized Urban Park. *Energy Rep.* **2020**, *6*, 1670–1684. [CrossRef]
17. Mayer, H.; Höppe, P. Thermal Comfort of Man in Different Urban Environments. *Theor Appl Clim.* **1987**, *38*, 43–49. [CrossRef]
18. Fanger, P.O. Thermal Comfort: Analysis and Applications in Environmental Engineering. In *Thermal Comfort: Analysis and Applications in Environmental Engineering*; Danish Technical Press: Copenhagen, Denmark, 1972; 244p.
19. Jendritzky, G.; De Dear, R.; Havenith, G. UTCI—Why Another Thermal Index? *Int. J. Biometeorol.* **2012**, *56*, 421–428. [CrossRef]
20. Zölch, T.; Rahman, M.A.; Pfleiderer, E.; Wagner, G.; Pauleit, S. Designing Public Squares with Green Infrastructure to Optimize Human Thermal Comfort. *Build. Environ.* **2019**, *149*, 640–654. [CrossRef]
21. Aboelata, A.; Sodoudi, S. Evaluating the Effect of Trees on UHI Mitigation and Reduction of Energy Usage in Different Built up Areas in Cairo. *Build. Environ.* **2020**, *168*, 106490. [CrossRef]
22. Teshnehdel, S.; Akbari, H.; Di Giuseppe, E.; Brown, R.D. Effect of Tree Cover and Tree Species on Microclimate and Pedestrian Comfort in a Residential District in Iran. *Build. Environ.* **2020**, *178*, 106899. [CrossRef]

23. Li, Y.; Lin, D.; Zhang, Y.; Song, Z.; Sha, X.; Zhou, S.; Chen, C.; Yu, Z. Quantifying Tree Canopy Coverage Threshold of Typical Residential Quarters Considering Human Thermal Comfort and Heat Dynamics under Extreme Heat. *Build. Environ.* **2023**, *233*, 110100. [CrossRef]

24. Binarti, F.; Koerniawan, M.D.; Triyadi, S.; Matzarakis, A. The Predicted Effectiveness of Thermal Condition Mitigation Strategies for a Climate-Resilient Archaeological Park. *Sustain. Cities Soc.* **2022**, *76*, 103457. [CrossRef]

25. Lai, D. Effects of Different Tree Layouts on Outdoor Thermal Comfort of Green Space in Summer Shanghai. *Urban Clim.* **2023**, *47*, 101398. [CrossRef]

26. Zhao, Y.; Chen, Y.; Li, K. A Simulation Study on the Effects of Tree Height Variations on the Façade Temperature of Enclosed Courtyard in North China. *Build. Environ.* **2022**, *207*, 108566. [CrossRef]

27. Yang, S.; Zhou, D.; Wang, Y.; Li, P. Comparing Impact of Multi-Factor Planning Layouts in Residential Areas on Summer Thermal Comfort Based on Orthogonal Design of Experiments (ODOE). *Build. Environ.* **2020**, *182*, 107145. [CrossRef]

28. Huang, K.-T.; Li, Y.-J. Impact of Street Canyon Typology on Building's Peak Cooling Energy Demand: A Parametric Analysis Using Orthogonal Experiment. *Energy Build.* **2017**, *154*, 448–464. [CrossRef]

29. Huang, X.; Yao, R.; Xu, T.; Zhang, S. The Impact of Heatwaves on Human Perceived Thermal Comfort and Thermal Resilience Potential in Urban Public Open Spaces. *Build. Environ.* **2023**, *242*, 110586. [CrossRef]

30. Xu, X.; Liu, S.; Sun, S.; Zhang, W.; Liu, Y.; Lao, Z.; Guo, G.; Smith, K.; Cui, Y.; Liu, W.; et al. Evaluation of Energy Saving Potential of an Urban Green Space and Its Water Bodies. *Energy Build.* **2019**, *188–189*, 58–70. [CrossRef]

31. Feng, L.; Yang, S.; Zhou, Y.; Shuai, L. Exploring the Effects of the Spatial Arrangement and Leaf Area Density of Trees on Building Wall Temperature. *Build. Environ.* **2021**, *205*, 108295. [CrossRef]

32. Yang, Y.; Zhou, D.; Wang, Y.; Meng, X.; Gu, Z.; Xu, D.; Han, X. Planning Method of Centralized Greening in High-Rise Residential Blocks Based on Improvement of Thermal Comfort in Summer. *Sustain. Cities Soc.* **2022**, *80*, 103802. [CrossRef]

33. Ouyang, W.; Morakinyo, T.E.; Ren, C.; Ng, E. The Cooling Efficiency of Variable Greenery Coverage Ratios in Different Urban Densities: A Study in a Subtropical Climate. *Build. Environ.* **2020**, *174*, 106772. [CrossRef]

34. Tian, Y.; Hong, B.; Zhang, Z.; Wu, S.; Yuan, T. Factors Influencing Resident and Tourist Outdoor Thermal Comfort: A Comparative Study in China's Cold Region. *Sci. Total Environ.* **2022**, *808*, 152079. [CrossRef] [PubMed]

35. Li, Y.; Hong, B.; Wang, Y.; Bai, H.; Chen, H. Assessing Heat Stress Relief Measures to Enhance Outdoor Thermal Comfort: A Field Study in China's Cold Region. *Sustain. Cities Soc.* **2022**, *80*, 103813. [CrossRef]

36. Lin, P.; Song, D.; Qin, H. Impact of Parking and Greening Design Strategies on Summertime Outdoor Thermal Condition in Old Mid-Rise Residential Estates. *Urban For. Urban Green.* **2021**, *63*, 127200. [CrossRef]

37. Liao, J. Evaluating the Vertical Cooling Performances of Urban Vegetation Scenarios in a Residential Environment. *J. Build. Eng.* **2021**, *39*, 102313. [CrossRef]

38. Willmott, C.J.; Robeson, S.M.; Matsuura, K. A Refined Index of Model Performance. *Int. J. Climatol.* **2012**, *32*, 2088–2094. [CrossRef]

39. Willmott, C.J. Some Comments on the Evaluation of Model Performance. *Bull. Am. Meteorol. Soc.* **1982**, *63*, 1309–1313. [CrossRef]

40. Morakinyo, T.E.; Lau, K.K.-L.; Ren, C.; Ng, E. Performance of Hong Kong's Common Trees Species for Outdoor Temperature Regulation, Thermal Comfort and Energy Saving. *Build. Environ.* **2018**, *137*, 157–170. [CrossRef]

41. Sun, C.; Lian, W.; Liu, L.; Dong, Q.; Han, Y. The Impact of Street Geometry on Outdoor Thermal Comfort within Three Different Urban Forms in Severe Cold Region of China. *Build. Environ.* **2022**, *222*, 109342. [CrossRef]

42. Salata, F.; Golasi, I.; Petitti, D.; de Lieto Vollaro, E.; Coppi, M.; de Lieto Vollaro, A. Relating Microclimate, Human Thermal Comfort and Health during Heat Waves: An Analysis of Heat Island Mitigation Strategies through a Case Study in an Urban Outdoor Environment. *Sustain. Cities Soc.* **2017**, *30*, 79–96. [CrossRef]

43. Lv, W.; Li, A.; Ma, J.; Cui, H.; Zhang, X.; Zhang, W.; Guo, Y. Relative Importance of Certain Factors Affecting the Thermal Environment in Subway Stations Based on Field and Orthogonal Experiments. *Sustain. Cities Soc.* **2020**, *56*, 102107. [CrossRef]

44. Taguchi, G.; Konishi, S. *Taguchi Methods, Orthogonal Arrays and Linear Graphs, Tools for Quality American Supplier Institute*; ASI Press: Hollywood, CA, USA, 1987.

45. Hwang, R.-L.; Lin, T.-P.; Liang, H.-H.; Yang, K.-H.; Yeh, T.-C. Additive Model for Thermal Comfort Generated by Matrix Experiment Using Orthogonal Array. *Build. Environ.* **2009**, *44*, 1730–1739. [CrossRef]

46. Liu, Z. Heat Mitigation Benefits of Urban Green and Blue Infrastructures: A Systematic Review of Modeling Techniques, Validation and Scenario Simulation in ENVI-Met V4. *Build. Environ.* **2021**, *200*, 107939. [CrossRef]

47. Bruse, M.; Fleer, H. Simulating Surface–Plant–Air Interactions inside Urban Environments with a Three Dimensional Numerical Model. *Environ. Model. Softw.* **1998**, *13*, 373–384. [CrossRef]

48. Skelhorn, C.; Lindley, S.; Levermore, G. The Impact of Vegetation Types on Air and Surface Temperatures in a Temperate City: A Fine Scale Assessment in Manchester, UK. *Landsc. Urban Plan.* **2014**, *121*, 129–140. [CrossRef]

49. Matzarakis, A.; Mayer, H.; Iziomon, M.G. Applications of a Universal Thermal Index: Physiological Equivalent Temperature. *Int. J. Biometeorol.* **1999**, *43*, 76–84. [CrossRef]

50. Chen, L.; Ng, E. Outdoor Thermal Comfort and Outdoor Activities: A Review of Research in the Past Decade. *Cities* **2012**, *29*, 118–125. [CrossRef]

51. Höppe, P. The Physiological Equivalent Temperature—A Universal Index for the Biometeorological Assessment of the Thermal Environment. *Int. J. Biometeorol.* **1999**, *43*, 71–75. [CrossRef]

52. He, X.; Miao, S.; Shen, S.; Li, J.; Zhang, B.; Zhang, Z.; Chen, X. Influence of Sky View Factor on Outdoor Thermal Environment and Physiological Equivalent Temperature. *Int. J. Biometeorol.* **2015**, *59*, 285–297. [CrossRef]

53. Morakinyo, T.E.; Kong, L.; Lau, K.K.-L.; Yuan, C.; Ng, E. A Study on the Impact of Shadow-Cast and Tree Species on in-Canyon and Neighborhood's Thermal Comfort. *Build. Environ.* **2017**, *115*, 1–17. [CrossRef]

54. Haghshenas, M.; Hadianpour, M.; Matzarakis, A.; Mahdavinejad, M.; Ansari, M. Improving the Suitability of Selected Thermal Indices for Predicting Outdoor Thermal Sensation in Tehran. *Sustain. Cities Soc.* **2021**, *74*, 103205. [CrossRef]

55. Fang, Z.; Zheng, Z.; Feng, X.; Shi, D.; Lin, Z.; Gao, Y. Investigation of Outdoor Thermal Comfort Prediction Models in South China: A Case Study in Guangzhou. *Build. Environ.* **2021**, *188*, 107424. [CrossRef]

56. Su, Y.; Zhao, Q.; Zhou, N. Improvement Strategies for Thermal Comfort of a City Block Based on PET Simulation— A Case Study of Dalian, a Cold-Region City in China. *Energy Build.* **2022**, *261*, 111557. [CrossRef]

57. Zhang, J.; Li, Z.; Hu, D. Effects of Urban Morphology on Thermal Comfort at the Micro-Scale. *Sustain. Cities Soc.* **2022**, *86*, 104150. [CrossRef]

58. Yang, Y.; Zhou, D.; Wang, Y.; Ma, D.; Chen, W.; Xu, D.; Zhu, Z. Economical and Outdoor Thermal Comfort Analysis of Greening in Multistory Residential Areas in Xi'an. *Sustain. Cities Soc.* **2019**, *51*, 101730. [CrossRef]

59. Niu, J.; Xiong, J.; Qin, H.; Hu, J.; Deng, J.; Han, G.; Yan, J. Influence of Thermal Comfort of Green Spaces on Physical Activity: Empirical Study in an Urban Park in Chongqing, China. *Build. Environ.* **2022**, *219*, 109168. [CrossRef]

60. Liu, Y.; Hu, J.; Yang, W.; Luo, C. Effects of Urban Park Environment on Recreational Jogging Activity Based on Trajectory Data: A Case of Chongqing, China. *Urban For. Urban Green.* **2022**, *67*, 127443. [CrossRef]

61. Deng, R.; Zhang, K.; Xu, J. Research on the temporal and spatial characteristics of urban park sports activities based on social media data. *J. Green Sci. Technol.* **2022**, *24*, 11–14. [CrossRef]

62. Qu, Y.; Zhang, R.; Wang, D. Study on the spatio-temporal characteristics of recreation behavior of the aged in urban open parks: Based on the investigation of the aged actives in summer and winter. *Archit. J.* **2016**, *S2*, 87–91.

63. Wang, C.; Wang, C.; Pan, H.; Yue, Y. Effect of Structure Parameters on Low Nitrogen Performance of Burner Based on Orthogonal Experiment Method. *Case Stud. Therm. Eng.* **2022**, *39*, 102404. [CrossRef]

64. Sawyer, S.F. Analysis of Variance: The Fundamental Concepts. *J. Man. Manip. Ther.* **2009**, *17*, 27E–38E. [CrossRef]

65. Freeman, J.V.; Campbell, M.J. The analysis of categorical data: Fisher's exact test. *Scope* **2007**, *16*, 1–12.

66. Ren, Q. *Optimum Design and Analysis of Experiments*, 2nd ed.; Higher Education Press: Beijing, China, 2003; ISBN 7-04-012736-9.

67. Huang, M.-L.; Hung, Y.-H.; Yang, Z.-S. Validation of a Method Using Taguchi, Response Surface, Neural Network, and Genetic Algorithm. *Measurement* **2016**, *94*, 284–294. [CrossRef]

68. Zhan, Q.; Xiao, Y.; Zhang, L.; Lin, Z.; Zou, Y.; Liao, W. Hygrothermal Performance Optimization of Lightweight Steel-Framed Wall Assemblies in Hot–Humid Regions Using Orthogonal Experimental Design and a Validated Simulation Model. *Build. Environ.* **2023**, *236*, 110262. [CrossRef]

69. Feng, J.; Yin, G.; Tuo, H.; Niu, Z. Parameter Optimization and Regression Analysis for Multi-Index of Hybrid Fiber-Reinforced Recycled Coarse Aggregate Concrete Using Orthogonal Experimental Design. *Constr. Build. Mater.* **2021**, *267*, 121013. [CrossRef]

70. Zhang, J.; Gou, Z. Tree Crowns and Their Associated Summertime Microclimatic Adjustment and Thermal Comfort Improvement in Urban Parks in a Subtropical City of China. *Urban For. Urban Green.* **2021**, *59*, 126912. [CrossRef]

71. Li, Z.; Zhang, H.; Juan, Y.-H.; Lee, Y.-T.; Wen, C.-Y.; Yang, A.-S. Effects of Urban Tree Planting on Thermal Comfort and Air Quality in the Street Canyon in a Subtropical Climate. *Sustain. Cities Soc.* **2023**, *91*, 104334. [CrossRef]

72. Xiao, J.; Yuizono, T. Climate-Adaptive Landscape Design: Microclimate and Thermal Comfort Regulation of Station Square in the Hokuriku Region, Japan. *Build. Environ.* **2022**, *212*, 108813. [CrossRef]

73. Morakinyo, T.E.; Lam, Y.F. Simulation Study on the Impact of Tree-Configuration, Planting Pattern and Wind Condition on Street-Canyon's Micro-Climate and Thermal Comfort. *Build. Environ.* **2016**, *103*, 262–275. [CrossRef]

74. Unal, M.; Uslu, C.; Cilek, A.; Altunkasa, M.F. Microclimate Analysis for Street Tree Planting in Hot and Humid Cities. *J. Digit. Landsc. Archit.* **2018**, *3*, 34–42.